Proceedings of the 8th World Congress on Mechanical, Chemical, and Material Engineering (MCM'22)
Prague, Czech Republic – July 31, 2022 - August 02, 2022
Paper No. HTFF 153
DOI: 10.11159/htff22.153

Influence of Contact Angle on the Internal Flow in a Freezing Water Droplet

Erik Fagerström[1], Anna-Lena Ljung[1]
[1]Luleå University of Technology
SE-97187 Luleå, Sweden
erik.fagerstrom@ltu.se; anna-lena.ljung@ltu.se

Abstract **–** Ice accretion upon a surface is of interest in areas such as wind power, electric power transmission and vehicles in cold climate. Ice assimilation appears when humid air or water droplets impacts and freezes on a cold surface. In the study presented in this paper, droplets are deposited onto aluminium plates constructed to generate a specific contact angle between the droplet and substrate. Five contact angles are investigated and Particle Image Velocimetry (PIV) is used to analyse the internal flow. The droplets are studied along the vertical centerline and at horizontal lines at distances of 50% and 75% of the total height of the droplet. From the results it is found that a lower contact angle will increase the magnitude of the internal flow close to the edges. A larger contact angle will instead increase the magnitude of the flow in the center of the droplet. For a droplet with lower contact angle it was furthermore found that there is a triangular area inside the droplet with close to zero velocity.

Keywords**:** Internal Flow, Freezing, Water Droplets, Particle Image Velocimetry

1. Introduction

Ice assimilation on a surface can lead to reduced efficiency and also dangers. The areas where it can be of interest is for example wind power [1]-[2], and in transportation such as airplanes, boats and cars. In the case of these examples ice is formed by humid air or impacting water droplets that starts to freeze on the surface.

For freezing water droplets there are generally two types of droplets that are studied. Either a sessile droplet that is resting on a surface [3]- [5] or an impacting droplet [6]- [8].

It was clearly shown by Huang et al. [3] that the contact angle influences the freezing process of a sessile droplet. It can then be of interest to further investigate how the contact angle influence the internal flow. In Fagerström et al. [9], a groove was used to control the contact radius, which in its turn controls the contact angle for droplets of equal volume. The results showed that a groove can be used to generate similar droplets for repeated experiments. This method allows the possibility to generate droplets of predetermined shape. The internal flow in a droplet is a part of the freezing process that has been less investigated. It was shown by Kawanami et al. [10] that temperature gradient, surface tension and buoyancy forces has an influence on the internal flow. Karlsson et al. [11]- [12] furthermore showed numerically that the internal natural convection and buoyancy forces are important for the internal flow. The Marangoni convection was however not accounted for in the simulations. It was later shown in experimental work by Karlsson et al. [13]- [14] that there is a directional change in the internal flow after a while. Voulgaropoulos et al. [15] used another method in their experiments. Covering the droplet surface with oil, the freezing was initiated from the interface and inwards instead of from the substrate. A directional change or upward movement could not be seen yet a downward motion was observed due to the downwards solidification from the top.

The setup used for the experiment in this study is based on the experimental setup in Karlsson et al. [13]- [14] with modifications made in Fagerström et al. [9].

The goal of this paper is to investigate how the internal flow is influenced by the shape of the droplet. Five aluminium plates with different outer groove radius are used to generate contact angles between 64.85° and 93.77°.

2. Material and Methods

First the experimental set-up is presented together with calculations of contact angle. The analysis method and uncertainty analysis is then presented.

2.1. Experimental setup

In the experiments, deionized (DI) water droplets with a volume of 10 µL are deposited on aluminium plates. The water droplets are seeded with fluorescent particles (microparticles GmbH PS-FlouRed) which has a diameter of 3.16µm. The aluminium plates are 50mm in diameter and have a thickness of 2mm. All plates have a circular groove that is 1mm deep. The inner radius of the groove is 0.765mm for all the plates while the outer radius varies for the different plates. Since aluminium have a higher thermal conductivity than ice, (238 $Wm^{-1}K^{-1}$ for aluminium to be compared with 2.1 $Wm^{-1}K^{-1}$ for ice [16]), the assumption is that the cooling will be similar for all the plates. The inner radius of the groove which is metal is the same even though the outer radius is varying i.e. the metal area is the same for all the studied cases while the ice area differs depending on the contact radius.

The outer radius of the groove will thus generate different contact angles which in turn changes the shape of the droplet. The contact angles are predetermined and the volume of the droplets are constant. Using equation

$$V = \frac{\pi}{6} h(3a^2 + h^2) \tag{1}$$

which is the volume for a spherical cap and the following equation to calculate the contact angle

$$\theta = 2 \cdot \arctan\left(\frac{h}{a}\right) \tag{2}$$

the height and the outer groove radius of the droplets can be determined theoretically. V is the volume of the droplet, h is the height from the surface to the top of the droplet, a is the surface radius of the droplet and θ is the contact angle. After manufacturing, the outer groove radius were measured for all plates to verify the radius. The theoretical surface radius and height is as seen in Table 1 together with the contact angle based on measurements of the aluminium plate.

Table 1: Theoretical shape of the droplet for the different plates.

Plate	A	B	C	D	E
Theoretical Contact Angle (°)	64.85	74.11	80.97	88.16	93.77
Surface Radius (mm)	2.0673	1.9208	1.8173	1.7110	1.6285
Height (mm)	1.3133	1.4502	1.5512	1.6569	1.7394
Experimental Contact Angle (°)	64.74	72.12	78.61	85.70	91.74

The PIV setup is the same as in Fagerström et al. [9], the DI droplet are released on the aluminium plate which is resting on an aluminium holder which is in turn cooled by a peltier element. The peltier element is cooled by water pumped from a tank with an ice/water mix. A plexiglass chamber is used to reduce external influences such as drafts. The chamber has four holes, one hole is placed in the back wall to give a clear view for the camera, and another hole is placed on the right side for the laser sheet to pass through. Two holes are also present on the top of the chamber, one for the hygrometer and one to insert the pipette to deposit the droplet. A Finnpipette F1 10µL, fastened on an optical rail, is used to release the droplets. To measure the temperature of the plate, a thermocouple type K model 6206000 are used. The fluorescent particles are lit up by a laser which enters the droplet at a perpendicular angle compared to the droplet.

2.2. Analysis and uncertainty of experiments

The water droplets are analysed by studying the movements of the particles at the center plane of the droplet. To find the velocity field of the droplet the Matlab package PIVlab was used. First the droplets boundary were defined in the program, secondly the PIV algorithm FFT were used and three passes was chosen, first 64x64, second 32x32 and third 16x16. A calibration of the velocity was derived based on the distance for a pixel and the time between the frames. After the velocity field has been found at the point in the freezing process that is of interest, it is imported into Matlab. In Matlab, an image analysis of the droplet at the chosen time is performed and the shape of the droplet is found by first using a threshold and then mark the general shape of the droplet to find the shape and coordinates for the liquid-gas interface. An issue with the liquid-gas interface, is that the light gets distorted. A method proposed by Kang et al. [17] upon which Minor et al. [18] did a correction, can be used to transform the velocity field from PIVlab to the correct

position in the droplet. This method has been used in previous experiments by Karlsson et al. [13]. Since there is a distortion of the velocity field information about the outermost part of the droplet is lost.

There are always some uncertainties with experiments, and the errors can be categorised into two subsections, systematic systematic errors and random errors. Examples of these can be for systematic errors; human influences such as small variations in droplet releases, reading of temperature, not enough mixed particles and offsets in PIVlab or image analysis of of the droplet. Random errors can be e.g. how the droplet attach to the groove, impact forces and that the freezing height in in the groove might have slight variations. The errors may thus lead to a slight change in contact angle and freezing time.

Fifteen experiments were performed for each plate, yet not all experiments were deemed valid. Only droplets with a base diameter within 2% of the grooves diameter were accepted in order to achieve uniform droplets. The valid experiments were then analysed three times to get an average for every experiment regarding the shape and internal flow.

3. Results and Discussion

In the presented results, the velocity is examined at 9% of the total freezing time. The velocities are studied at three positions inside the droplet, i.e. the vertical centerline, and two horizontal lines at 50% and 75% of the droplets height. The locations for the vertical and horizontal lines can be seen in Figure 1. For the horizontal cases the total velocity is studied as well as the separate components in the x- and y-direction. It is assumed that the velocity field in a droplet is symmetrical around the centerline even though the internal flow at the right side and the left side of the vertical line through the droplet will differ slightly in the experimental results. The difference between the two edges is due to the laser sheet coming in from the left. It will create an area along the right edge that is less illuminated due to refraction from the liquid-gas interface. This makes the movement along the right edge less certain since the PIV analysis might show errors in that area. The most focus in the result sections will therefore be on the left side of the vertical centerline.

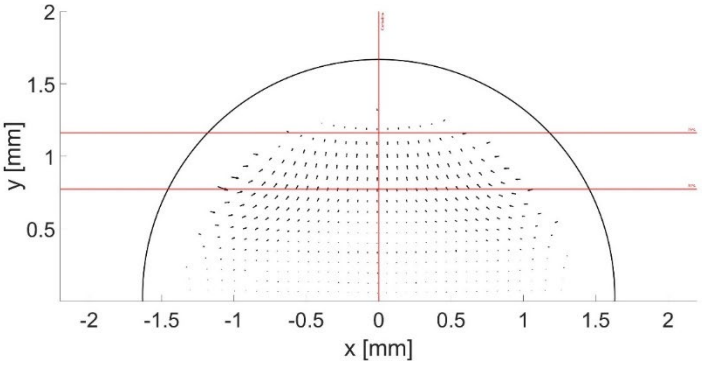

Figure 1: The locations where the velocity is investigated. Along the vertical centerline and at horizontal lines at 75% and at 50% from the surface.

3.1 Velocity Along the Vertical Centerline

From Figure 2 it is seen that a higher contact angle will give a higher velocity along the centerline. The peak of the velocities are found between 73.5-80% of the droplets heights for all the plates. From the centerline velocities displayed in Figure 2, it can be seen that there is a scatter of the velocities close to the substrate and this phenomena is known to stem from the ice layer. The ice layer at 9% of the freezing time is around 40% of the height for all the plates. It is difficult to determine the exact location, since both visually and in the velocity field there is a triangular area of less movement in the middle of the droplet, which will be discussed more in the following sections.

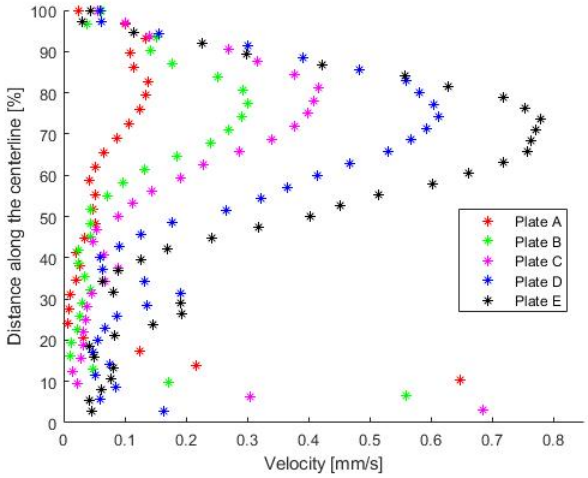

Figure 2: The velocity along the centerline for the five different plates at 9% of the total freezing time.

3.2. Velocity Along the Horizontal Line

First the total velocity will be discussed and in conjunction to the total velocity, also the velocities in x- and y-direction are investigated individually.

3.2.1 Total Velocity

In this subsection the total velocity along horizontal lines at 75% and 50% of the droplet height is studied. Looking at Figure 3a, which is at 75% of the droplets height, the highest internal velocity is found in the center for droplets with high contact angle (i.e. plate D and E). Droplets with smaller contact angle (plate A, B) will on the contrary show the highest velocity close to the liquid-gas interface. Interestingly, droplet type C, with a theoretical contact angle of 80.97°, follows the behaviour of low contact angle droplets in the center, and the behaviour of high contact angle at the edges.

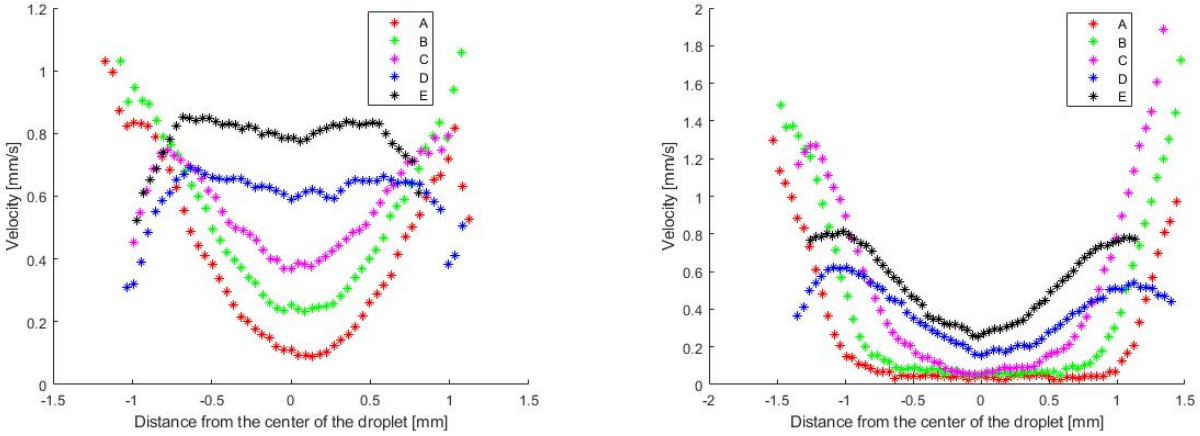

(a) The total velocity at a horizontal line at 75% along the vertical centerline from the surface.

(b) The total velocity at a horizontal line at 50% along the vertical centerline from the surface.

Figure 3: The total velocity at a horizontal line at (a) 75% and (b) 50% along the vertical centerline of the droplet from the surface.

Droplet type A, which has the smallest contact angle, has hardly any velocity in the middle of the droplet. Looking at Figure 3b, which displays the velocity at 50% of the droplets height, it is seen that there is barely any movement in the span of -0.6mm to 0.6mm for this droplet size. This is the earlier mentioned triangular area with very small velocities in the droplet. In the same Figure 3b, plate B also has barely any internal flow at the 50% height in the span of -0.5mm to 0.5mm while plate C has almost zero just at the centerline point and not in a span. Looking instead at the edges, plate A, B and C have significant higher velocity compared to plate E and D, which instead show a somewhat higher velocity in the middle.

3.2.2 Velocity in y-direction

As for the y-direction along the horizontal line at 75% of the droplet height as seen in Figure 4a, the velocity is rather constant in the middle of the droplet and all contact angles show a lower velocity towards the edge of the droplet. It can be seen that the difference in magnitude between a higher and lower contact angle is almost a factor of 10 between plate E and A. In the middle of the droplets at 50% of the vertical height, Figure 4b, plate A and B show close to zero movement in the y-direction and plate C has a very low velocity. Closer towards the edge it can be seen that plate C and B have higher y-velocities than plate E and D. This indicates that the flow closer to the top (i.e. at 75% of the droplet height) is more uniform in the y direction. At 50% it is then seen that a flatter droplet with a lower contact angle will have a larger velocity at the droplet edge than for a droplet with a higher contact angle.

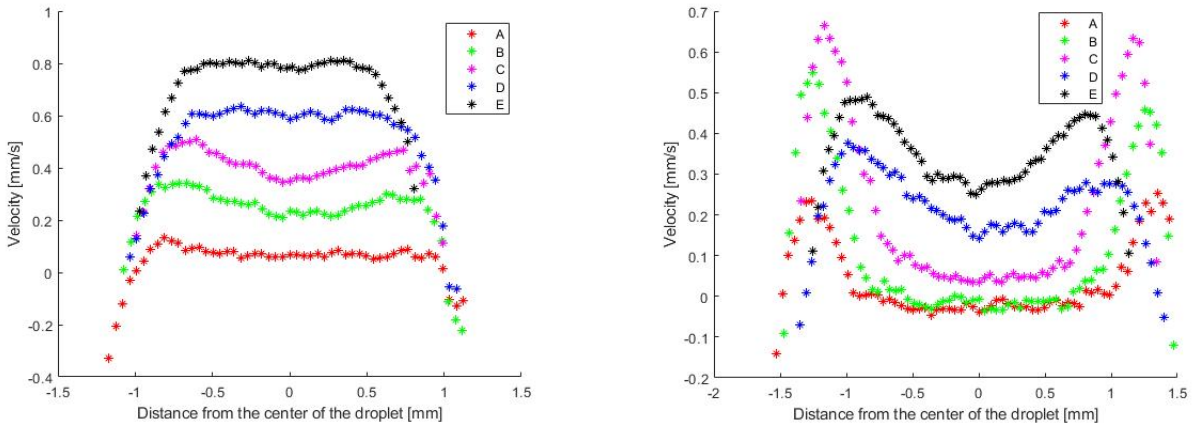

(a) The y velocity at a horizontal line at 75% along the vertical centerline from the surface.

(b) The y velocity at a horizontal line at 50% along the vertical centerline from the surface.

Figure 4: The y velocity at a horizontal line at (a) 75% and (b) 50% along the vertical centerline of the droplet from the surface.

3.2.3 Velocity in x-direction

In Figure 5a, the x component is shown for a horizontal line at 75% of the droplets height. It can be seen that all plates have an internal flow inwards towards the center. Droplets on plate A and B have a higher x velocity at the edges then the droplets with a higher contact angle. The difference is almost a factor of two. In Figure 5b, which displays the velocity in the x-direction at 50% of the height, it can be seen as well that plate A, B and C have a higher velocity close to the droplet edge. For plate A, there is barely any movement in the x-direction in the span -1mm to 1mm at 50%. Plate B have a similar area of hardly any movement but it is significant smaller. Plate D and E have more of a linear relationship at both 75% and 50%.

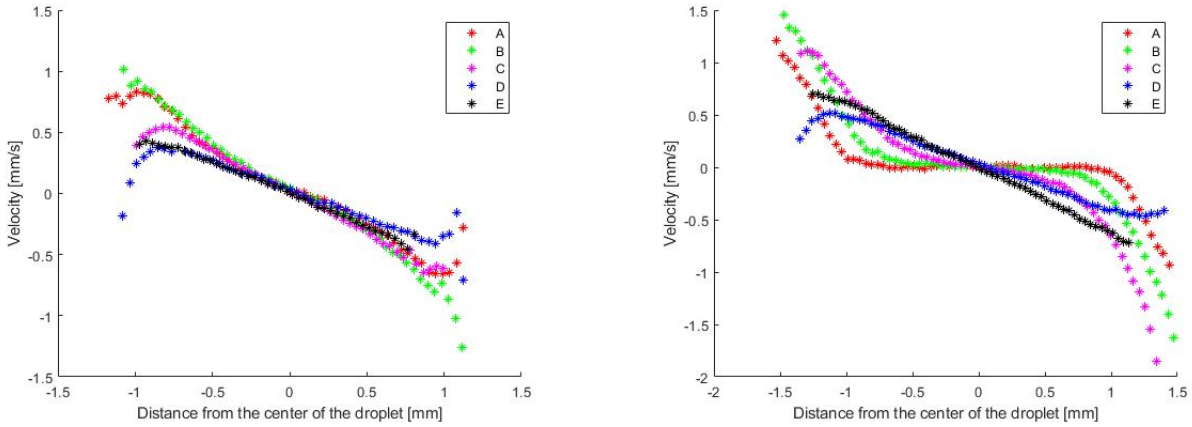

(a) The x velocity at a horizontal line at 75% along the vertical centerline from the surface.

(b) The x velocity at a horizontal line at 50% along the vertical centerline from the surface.

Figure 5: The x velocity at a horizontal line at (a) 75% and (b) 50% along the vertical centerline of the droplet from the surface.

3.3 Vector Field

As mentioned in the previous sections, droplets in the lower range of contact angles show a triangular stagnation area with only very small velocities. For comparison, Figure 6a and 6b shows the vector fields of the internal flow of droplet type A and E after the correction method has been applied and the ice layer removed. Starting with Figure 6a for plate type A, it can be seen that the internal flow has a high velocity at the edge and that there is a triangular shaped area in the middle where the velocity vectors are quite small. Then comparing with Figure 6b representing plate type E, the internal flow is higher in the center with a lower velocity along the edges. A small triangular shaped area is displayed also for droplet type E, but it is much smaller when compared to plate A.

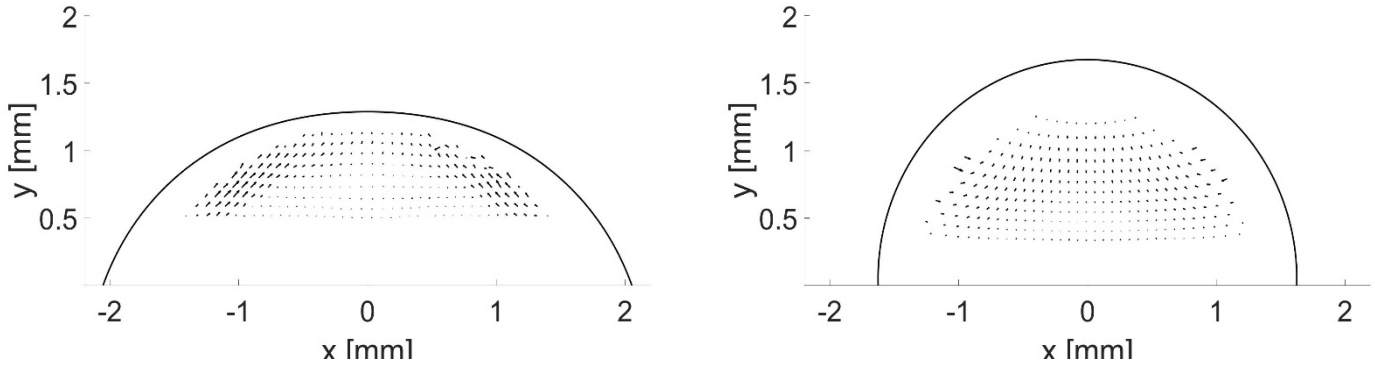

(a) The vector field after the correction method is applied and the ice is removed for a droplet on plate A.

(b) The vector field after the correction method is applied and the ice is removed for a droplet on plate E.

Figure 6: The vector field after the correction method is applied and the ice is removed for (a) plate A and (b) plate E.

4. Conclusion

In this paper the internal flow along the vertical centerline and at two horizontal lines are investigated. Both the total total velocity and the x and y components are investigated for the horizontal lines. From this analysis, it can be found that a that a droplet with a lower contact angle (i.e. a flatter droplet) will show the highest velocities close to the liquid-gas interface. interface. A droplet with a higher contact angle (i.e. a more spherical droplet) will in turn show the highest velocities along along the vertical centerline and lower magnitudes at the edges. It was also found that for a droplet with a lower contact angle, a triangular area appear in the center where there is barely any movement.

Acknowledgements

We like to acknowledge all the help provided by Dr. Henrik Lycksam for the help of setting up the experimental setup.

References

[1] R. S. Myong, "Atmospheric Icing Effects On Aerodynamics Of Wind Turbine Blade," In *Asme International Mechanical Engineering Congress And Exposition*, San Diego, 2013.

[2] A. Faizan And V. S. Muhammad, "Review Of Icing Effects On Wind Turbine In Cold Regions," In *E3s Web Of Conferences*, 2018.

[3] L. Huang, Z. Liu, Y. Liu, Y. Gou And L. Wang, "Effect Of Contact Angle On Water Droplet Freezing Process On A Cold Flat Surface," *Experimental Thermal And Fluid Science,* Vol. 40, Pp. 74-80, 2012.

[4] F. Tavakoli, S. H. Davis And H. P. Kavehpour, "Freezing Of Supercooled Water Drops On Cold Solid Substrates: Initiation And Mechanism," *Journal Of Coatings Technology And Research,* Vols. 869-875, No. 5, P. 12, 2015.

[5] L. Menglong, S. Mengjie, M. Zhenjun, W. Xiaotao And Z. Long, "A Modeling Study Of Sessile Water Droplet On The Cold Plate Surface During Freezing Under Natural Convection With Gravity Effect Considered," *International Journal Of Multiphase Flow,* Vol. 143, P. 103749, 2021.

[6] Z. Jin , H. Zhang And Z. Yang, "Experimental Investigation Of The Impact And Freezing Processes Of A Water Droplet On An Ice Surface," *International Journal Of Heat And Mass Transfer,* Vol. 109, Pp. 716-724, 2017.

[7] Z. Jin, H. Zhang And Z. Yang, "The Impact And Freezing Processes Of A Water Droplet On Different Cold Cylindrical Surfaces," *International Journal Of Heat And Mass Transfer,* Vol. 113, Pp. 318-323, 2017.

[8] X. Zhang, X. Liu, X. Wu And J. Min, "Impacting-Freezing Dynamics Of A Supercooled Water Droplet On A Cold Surface: Rebound And Adhesion," *International Journal Of Heat And Mass Transfer,* Vol. 158, P. 119997, 2020.

[9] E. Fagerström, A.-L. Ljung, L. Karlsson And H. Lycksam, "Influence Of Substrate Material On Flow In Freezing Water Droplets—An Experimental Study," *Water,* Vol. 13, No. 12, P. 1628, 2021.

[10] T. Kawanami, M. Yamada, S. Fukusako And H. Kawai, "Solidification Characteristics Of A Droplet On A Horizontal Cooled Wall," *Heat Transfer-Japanese Research: Co-Sponsored By The Society Of Chemical Engineers Of Japan And The Heat Transfer Division Of Asme,* Vol. 26, No. 7, Pp. 469-483, 1997.

[11] L. Karlsson, A.-L. Ljung And S. Lundström, "Influence Of Internal Natural Convection On Water Droplets Freezing On Cold Surfaces," In *Proceedings Of Conv-14: International Symposium On Convective Heat And Mass Transfer*, 2014.

[12] L. Karlsson, A.-L. Ljung And S. T. Lundström, "Modelling The Dynamics Of The Flow Within Freezing Water Droplets," *Heat And Mass Transfer,* Vol. 54, No. 12, Pp. 3761-3769, 2018.

[13] L. Karlsson, H. Lycksam, A.-L. Ljung, P. Gren And S. T. Lundström, "Experimental Study Of The Internal Flow In Freezing Water Droplets On A Cold Surface," *Experiments In Fluids,* Vol. 60, No. 12, Pp. 1-10, 2019.

[14] L. Karlsson, A.-L. Ljung And S. T. Lundström, "Comparing Internal Flow In Freezing And Evaporating Water Droplets Using Piv," *Water,* Vol. 12, No. 5, P. 1489, 2020.

[15] V. Voulgaropoulos, M. Kadivar, M. A. Moghimi, M. Maher, H. Alawadi, O. K. Matar And C. N. Markides, "A Combined Experimental And Computational Study Of Phase-Change Dynamics And Flow Inside A Sessile Water Droplet Freezing Due To Interfacial Heat Transfer," *International Journal Of Heat And Mass Transfer,* Vol. 180, P. 121803, 2021.

[16] C. Nordling And J. Österman, Physics Handbook For Science And Engineering, Lund, Sweden: Studentlitteratur Ab, 2006.

[17] K. H. Kang, S. J. Lee, C. M. Lee And I. S. Kang, "Quantitative Visualization Of Flow Inside An Evaporating Droplet Using The Ray Tracing Method," *Measurement Science And Technology,* Vol. 15, No. 6, P. 1104, 2004.

[18] G. Minor, P. Oshkai And N. Djilali, "Optical Distortion Correction For Liquid Droplet Visualization Using The Ray Tracing Method: Further Considerations," *Measurement Science And Technology,* Vol. 18, No. 11, P. L23, 2007.